

# EXCELLENT REAR SIDE PASSIVATION ON MULTI-CRYSTALLINE SILICON SOLAR CELLS WITH 20 NM UNCAPPED $\text{Al}_2\text{O}_3$ LAYER: INDUSTRIALIZATION OF ALD FOR SOLAR CELL APPLICATIONS

I. Cesar<sup>1</sup>, E. Granneman<sup>2</sup>, P. Vermont<sup>2</sup>, E. Tois<sup>3</sup>, P. Manshanden<sup>1</sup>, L.J. Geerligs<sup>1</sup>, E. E. Bende<sup>1</sup>, A.R. Burgers<sup>1</sup>, A.A. Mewe<sup>1</sup>, Y. Komatsu<sup>1</sup>, A.W. Weeber<sup>1</sup>

1) ECN Solar Energy, P.O. Box 1, 1755 ZG Petten, The Netherlands, corresponding author: cesar@ecn.nl

2) Levitech BV, Luidsprekerstraat 1, 1322AW Almere, The Netherlands

3) ASM Microchemistry ltd., Väinö Auerin Katu 12 A 00560 Helsinki, Finland

## ABSTRACT

Current bottlenecks for industrialization of  $\text{Al}_2\text{O}_3$  deposited by Atomic Layer Deposition (ALD) for crystalline silicon solar cell applications are low growth rate and stability of thin and uncapped layers during co-firing. First results on the performance of a high throughput ALD proto-type, the Levitrack, are presented. Excellent passivation properties have been obtained after firing, for 12 nm thick films deposited on p-Cz (2.3  $\Omega\cdot\text{cm}$ ) with  $S_{\text{eff}} < 15\text{cm/s}$  ( $\Delta n = 3 \times 10^{15}\text{cm}^{-3}$ ). These layers are compatible with solar cells that operate at a maximum open-circuit voltage of 720mV. Furthermore, we report on the passivation of 20nm uncapped aluminum oxide layers on the rear of p-type mc-Si bifacial cells. LBIC measurements unveiled excellent passivation properties on areas covered by 20nm of  $\text{Al}_2\text{O}_3$  characterized by an IQE of 91% at 980nm. Remarkably, these lifetime and cell results were obtained without lengthy post-treatments like forming gas anneal.

## INTRODUCTION

Aluminium oxide has received much attention in recent years because of its potential surface passivation performance in silicon solar cells. It is known to passivate boron emitters [1] and can be applied as rear dielectric in rear passivated solar cells based on p-type wafers, like the PERC [2]. Surface passivation levels at  $\text{Al}_2\text{O}_3$  layers expressed by values below 10 cm/s for the effective surface recombination velocity,  $S_{\text{eff}}$ , are commonly reported. The reduced recombination at the surface is brought about by field effect as well as chemical passivation. This dielectric is characterized by very high negative surface density ( $10^{12}$  -  $10^{13}\text{cm}^{-2}$ ) [3] [4] that repel electrons from the surface, reducing the chance for recombination with holes. A major advantage of the negatively charged  $\text{Al}_2\text{O}_3$  on p-type surfaces is that it does not cause inversion layer shunting. This phenomenon severely reduces the  $J_{\text{sc}}$  of rear passivated solar cells and is commonly observed for positively charged dielectrics such as  $\text{SiN}_x$  [5;6]. Although  $\text{Al}_2\text{O}_3$  has proven its potential as effective rear dielectric in high efficiency solar cells (> 20%) [2], its application in industry is impeded by several factors: 1) low wafer throughput rates related to the deposition method and lengthy anneals, 2) firing stability and 3) contact formation through the dielectric. Industrial deposition methods for  $\text{Al}_2\text{O}_3$  with higher deposition rates such as RF sputtering and PECVD, rely on long annealing

steps (~25min) in nitrogen or forming gas (FGA) atmosphere to achieve reasonable surface recombination velocities of 55cm/s [7] and 2.9 cm/s [4]. Excellent passivation quality is commonly reported for  $\text{Al}_2\text{O}_3$  grown by atomic layer deposition [3] [8] [9]. This technique is characterized by a low deposition rate in the order of 1-2 nm/min and is handled in a wafer-by-wafer mode which is typically operated on laboratory scale. Recently, Schmidt et al [9] reported lifetime values as high as 1.4ms ( $S_{\text{eff}}$  of 6 cm/s) for 30nm thick  $\text{Al}_2\text{O}_3$  layers on 1.5 $\Omega\cdot\text{cm}$  p-Si after a forming gas anneal treatment (15 min at 425C). A firing step (830°C, 3sec) that is commonly applied in industry for screen-printed solar cells decreased the effective lifetime ( $\tau_{\text{eff}}$ ) to about 300 $\mu\text{s}$ . The magnitude of firing degradation increased for thinner wafers down to lifetimes of 50  $\mu\text{s}$  for 3.6nm thick films. Capping the thin  $\text{Al}_2\text{O}_3$  layer with a 70nm thick  $\text{SiN}_x$  layer improved the firing stability resulting in a lifetime of 300  $\mu\text{s}$  ( $S_{\text{eff}}$  of 44cm/s). As this firing step generally increases the surface recombination velocity of  $\text{Al}_2\text{O}_3$  layers, the main challenge for the industrialization of  $\text{Al}_2\text{O}_3$  is to develop a simple and high throughput process for  $\text{Al}_2\text{O}_3$  deposition that maintains reasonable levels of passivation after firing. The discussed measures to improve the firing stability by capping the  $\text{Al}_2\text{O}_3$  layer, as well as the application of long anneals steps, are unfavorable for industrialization. We report on the excellent performance of uncapped ALD  $\text{Al}_2\text{O}_3$  films with a thickness of 20nm in solar cells without forming gas anneal. Additionally, we report on the performance after firing of thin and uncapped  $\text{Al}_2\text{O}_3$  layers deposited for the first time by a prototype of an industrial and high-throughput ALD system, the Levitrack, developed by Levitech.

## EXPERIMENTAL SECTION

In order to assess the potential for industrial rear side passivation of uncapped  $\text{Al}_2\text{O}_3$  layers, two different ALD setups were used to deposit  $\text{Al}_2\text{O}_3$  layers: 1) the Levitrack from Levitech B.V. which operates in a continuous in-line processing mode and 2) F450 ALD from ASM microchemistry ltd. which operates in a non-continuous wafer-by-wafer mode. Mirror polished mono-crystalline wafers were double-side coated by both systems for minority carrier lifetime measurements (WCT-120 Silicon Wafer Lifetime Tester, Sinton Consultancy). The lifetime was measured directly after deposition as well as after a rapid firing step (few seconds,  $T_{\text{peak}}$  about 800°C) that is typically used for contact formation in screen-printed solar cells. Also the influence of a  $\text{N}_2$  and forming gas (5%  $\text{H}_2$  / 95% $\text{N}_2$ ) anneal step of 25min is investigated. All mono-crystalline wafers received a thorough

cleaning step[10] prior to deposition. The performance of the Al<sub>2</sub>O<sub>3</sub> layer deposited by the F450 ALD was also tested on cell level.

### Levitrack: industrial deposition of ALD Al<sub>2</sub>O<sub>3</sub> films

The basic principle of the system is shown in Figure 1. The wafers are floating in a linear gas track; N<sub>2</sub> and N<sub>2</sub>/precursor mixtures are injected from the top wall downwards onto the wafers, while at the bottom only N<sub>2</sub> is introduced. The combination of a narrow gap (0.15mm) and a relatively large gas flow of a few slm above and below each of the wafers results in a robust transport of wafers in the track. This arrangement ensures that the wafers do not touch the top and bottom walls of the reaction chamber. Special precautions are taken to guarantee that the wafers also do not collide with the side walls of the track.

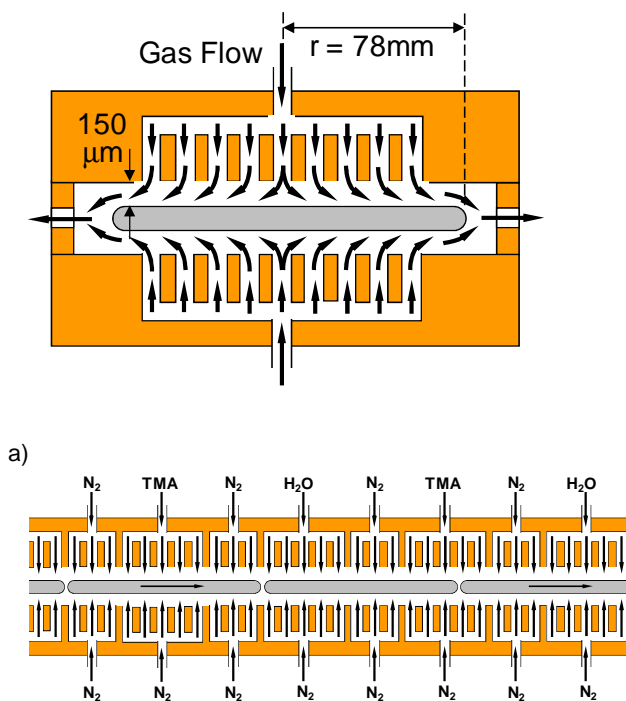


Figure 1, Levitrack system, a high-throughput ALD system (developed by Levitech, patents pending). The wafers float in gas injected into the transport chamber through holes in the top and bottom walls. Each sequence of TMA-N<sub>2</sub>-H<sub>2</sub>O-N<sub>2</sub> results in the deposition of a saturated (mono-) layer of Al<sub>2</sub>O<sub>3</sub> on one side of the wafer. a) and b) cross sections in directions perpendicular and parallel to the wafer transport direction, respectively.

Each time a wafer passes a cell containing a TMA-N<sub>2</sub>-H<sub>2</sub>O-N<sub>2</sub> gas injection sequence, a saturated ALD Al<sub>2</sub>O<sub>3</sub> layer is deposited. The total number of cells in the track determines the final Al<sub>2</sub>O<sub>3</sub> film thickness on all wafers. For the first systems a film thickness of 10-12nm is targeted (~100 cells). The system is designed to operate in a

temperature window of 150-300°C and to process wafers with a throughput up to 1 wafer/s (3600 wafers/hr).

The characteristics of the Levitrack approach are the following: as the TMA and H<sub>2</sub>O precursor flows are strictly separated in space (in case of a fully loaded track as well as in case of an empty track), there is no deposition of Al<sub>2</sub>O<sub>3</sub> films on the walls of the track. This will have a very positive impact on the maintenance aspects of the system. Further, when precursors are injected from one wall only (top or bottom), deposition will take place on only one side of the wafer. In addition to that, as the gap between wafer and walls is only 0.15mm, heating of the wafer is very fast; the wafer will be heated to process temperature in a matter of seconds. Finally, as the process is at atmospheric pressure, no vacuum pumps are present; the Levitrack system is made entirely from aluminum, and does not have any moving parts.

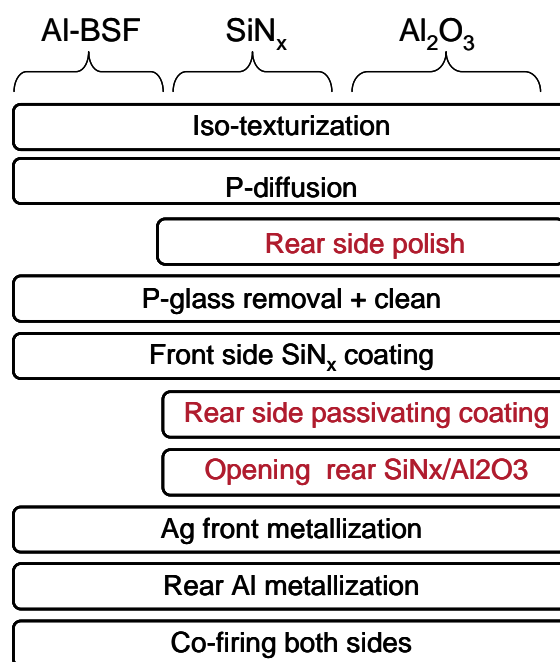


Figure 2, process flow of Al-BSF reference, SiNx and Al<sub>2</sub>O<sub>3</sub> passivated cells. The clean used is a thorough clean procedure that affects both the front and rear side [10;11].

A series of layer thicknesses was deposited on p-Si Cz wafers (150mm, 2.3 Ω.cm) in the 2m long gas track of the Levitech proto-type. A single run at a deposition temperature of 200°C resulted in an Al<sub>2</sub>O<sub>3</sub> layer thickness of about 2 nm. As the Levitrack currently operates in single side deposition mode (precursors only flow from top), double side deposition of the layer thicknesses 5, 12, 18 and 24 nm were achieved by multiple deposition runs through the gas track while flipping the wafer after each run. As a consequence, one unpassivated side of each wafer was exposed to the handling and thermal treatment of its first run. This might have a negative effect on

the final surface passivation quality for the symmetric test-structures. However, this does not pose a problem for future cell processing as the front side can be coated by SiNx prior to the rear side deposition or the Levitrack can be modified to operate in double side deposition mode.

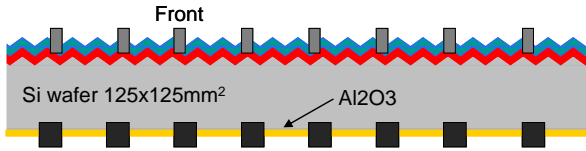


Figure 3, open cell concept with metal print on rear (50 fingers, 2.5 mm pitch, 2 busbars). Top down: Ag contacts, SiN coating front, texture, emitter, p-type bulk, Al<sub>2</sub>O<sub>3</sub> or SiNx as passivating coating on rear (yellow) + Al-metal contacts (black). Same structure is applied for SiN rear side passivation.

### F450 ALD labscale Al<sub>2</sub>O<sub>3</sub> deposition

The 20nm thick Al<sub>2</sub>O<sub>3</sub> films for the lifetime and the solar cell study were deposited in a flow type F-450 atomic layer deposition (ALCVD) reactor (ASM Microchemistry Ltd.). The reaction temperature was 300°C. Trimethylaluminum (=TMA), (CH<sub>3</sub>)<sub>3</sub>Al, and water were used as precursor chemicals. The growing of the films was carried out with the aid of alternating the TMA and water pulses. Between the pulses the reaction space was purged carefully so that the source would not be simultaneously in the reaction chamber. As only one side of the wafer is exposed to the precursors during deposition, double side deposition was achieved in a second run after turning the wafer.

We evaluated the performance of the Al<sub>2</sub>O<sub>3</sub> layer obtained from the F450 ALD system as rear dielectric in a PASHA cell (Passivated on all side H-pattern) by comparing it to that of SiNx and to a conventional full Al-BSF cell. All solar cells are prepared with 180 micron thick p-type silicon wafer (125x125mm<sup>2</sup>, 1-1.5 ohm.cm). The preparation method of the double side SiNx passivated solar cells as well as the full Al-BSF reference cells investigated in this work, are similar to that of our previous report with two exceptions<sup>1)</sup> for the Al<sub>2</sub>O<sub>3</sub> rear side passivated cells the rear SiNx was replaced by Al<sub>2</sub>O<sub>3</sub>; and 2) the rear dielectric layers were chemically opened by screen printing prior to metallization<sup>6;11</sup>. The process flow is illustrated in Figure 2. It is important to mention that no forming gas anneal was performed in this experiment to activate the Al<sub>2</sub>O<sub>3</sub> passivation and that a typical firing step (T<sub>peak</sub> about 800°) was performed. The rear metallization designs consist of an H-pattern with 2.5 mm pitched and 470 micron wide fingers which were wider than the opened area in the dielectric. The large rear contact spacing as compared to PERC (~ 1mm) is used to enable passivation studies by means of LBIC mapping such as presented in this work. Front and rear contacts are prepared by screen printing

silver or aluminum based pastes. The emitter of the Al-BSF cells was isolated by grinding the edges after firing.

The details of the performed experiments such as the ALD system and deposition temperature, wafer resistivity and deposited Al<sub>2</sub>O<sub>3</sub> layer thickness are summarized in Table 1.

**Table 1, Overview experiments: Deposition parameters, Al<sub>2</sub>O<sub>3</sub> layer thickness, sample structure and material.**

Deposition parameters	Lifetime test structure (double side deposition)	PASHA Cell (Rear side deposition)
F450 ALD T <sub>dep</sub> =300°C Wafer by wafer mode	100mm p-Si Fz 1.8 Ω.cm 20nm Al <sub>2</sub> O <sub>3</sub>	125mm, p-Si mc, 1-1.5 Ω.cm 20nm Al <sub>2</sub> O <sub>3</sub>
Levitrack ALD T <sub>dep</sub> =200°C Continuous process	150mm p-Si Cz, 2.3 Ω.cm 5, 12, 18, 24 nm Al <sub>2</sub> O <sub>3</sub>	

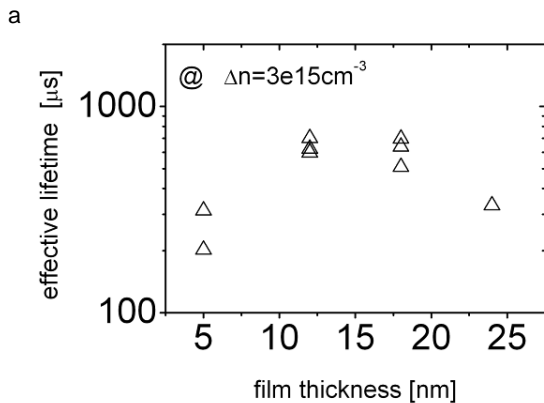
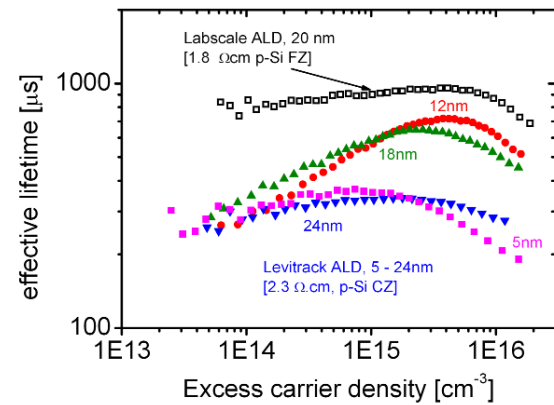
## RESULTS AND DISCUSSION

### Lifetime performance

First depositions of Al<sub>2</sub>O<sub>3</sub> on p-type Cz-Si (2.3 Ωcm) obtained from the Levitrack system yielded excellent passivation quality after firing. As deposited, these layers had very low lifetimes while the firing step activated the surface passivation quality to excellent levels as illustrated in Figure 4 a. For films with layer thicknesses of 5, 12, 18 and 24 nm τ<sub>eff</sub> of 313, 702, 633 and 332 μs were measured at Δn=3e15cm<sup>-3</sup>. The dependence of the τ<sub>eff</sub> on the film thickness is illustrated in Figure 4 b, and clearly shows an optimum between 12 and 18nm. Similar values were obtained after a forming gas or nitrogen anneal during 25min at 425°C. Reasonable repeatability has been obtained by performing multiple equal depositions (duplo) as can be judged from Figure 4 b. The best lifetime for the 12nm thick layer correspond to a surface recombination velocity of 15cm/s assuming a 4ms bulk lifetime. This level of passivation is compatible with a maximum open circuit voltage in solar cells of 720mV<sup>[12]</sup> for 1.5 Ω.cm p-Si, and is slightly better than the 695mV reported by Schmidt et al. for the same wafer resistivity, obtained for 3.6nm thick Al<sub>2</sub>O<sub>3</sub> layer with a 75nm capping layer after FGA and firing. It should be noted that directly after firing even higher lifetimes were measured for the Levitrack as well as the F450 ALD samples. The lifetime stabilized after two days to the levels presented in Figure 4 a and b. The lifetimes of the F450 ALD sample presented in the same figure was measured after nearly a year, which demonstrates the long term stability in dark.

Lifetime measurements of samples deposited by the F450 ALD system that received a 20nm thick layer of Al<sub>2</sub>O<sub>3</sub> showed reasonable results as deposited which even improved after

firing. At an injection level of  $3e15\text{cm}^{-3}$  the as-deposited life times ranged between 175 and 340 $\mu\text{s}$  while the firing increased the life times up to 942  $\mu\text{s}$ . The lifetime after firing corresponds to a value for  $S_{\text{eff}}$  of 10 cm/s assuming a bulk lifetime of 4 ms. The best obtained  $\tau_{\text{eff}}$  as function of injection density is illustrated in Figure 4. The fact that the 18nm thick Levitrack sample shows lower lifetimes as compared to the 20nm thick F450 sample could be related to the handling of the first run as the uncoated surface of the second run might no longer have the same properties as that of the first run.



b  
Figure 4, (a) Measured  $\tau_{\text{eff}}$  as function of injection density  $\Delta n$  on p-type FZ-Si measured 1 year after firing with double side coated  $\text{Al}_2\text{O}_3$  deposited in lab-scale ALD system (F-450, on 1.8  $\Omega\text{cm}$ , open markers) and industrial ALD system (Levitrack, on 2.3  $\Omega\text{cm}$ , closed markers) measured after 2 days. Four  $\text{Al}_2\text{O}_3$  layer thicknesses of 5, 12, 18 and 24nm were deposited in the Levitrack and no forming gas nor nitrogen anneal was performed. (b)  $\tau_{\text{eff}}$  measured 2 day after firing at  $\Delta n=3e15\text{cm}^{-3}$  as function of film thickness of  $\text{Al}_2\text{O}_3$  deposited in Levitrack (multiple samples obtained under equal conditions).

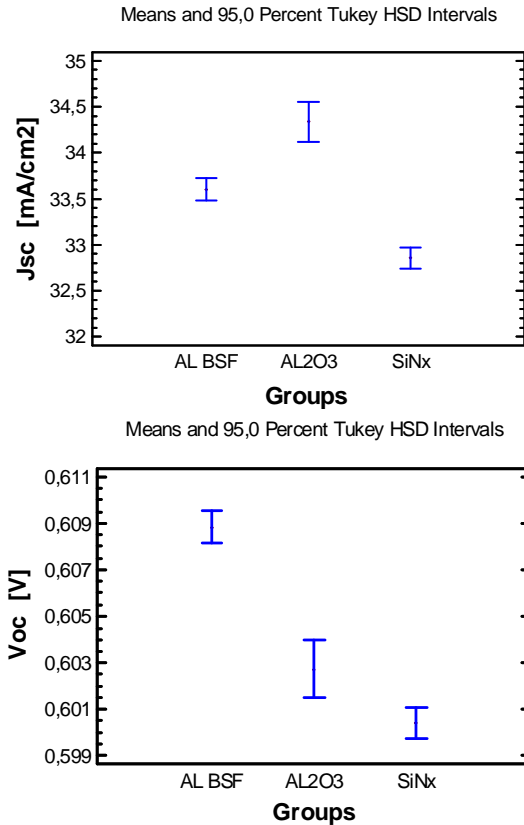


Figure 5,  $V_{\text{oc}}$  (a) and  $J_{\text{sc}}$  (b) comparison of  $\text{Al}_2\text{O}_3$  and  $\text{SiNx}$  rear passivated solar cells of the PASHA type with the conventional full area Al-BSF H-pattern cell with a full area Al-BSF. Groups consist of neighboring mc wafers.

### Cell performance

The PASHA type solar cells prepared with the  $\text{Al}_2\text{O}_3$ , clearly outperform the PASHA cells that are passivated by  $\text{SiNx}$  and, as will be shown later, performance is limited due to poor passivation at the metal rear leads compared to the full area BSF reference. In this paper, the analysis of the IV response will be focused on the  $V_{\text{oc}}$  and  $J_{\text{sc}}$  as the rear metallization (H-) pattern of the PASHA cell is not optimized to minimize resistive losses. The fill factors of all passivated groups were above 70% which ensures that  $J_{\text{sc}}$  and  $V_{\text{oc}}$  are not compromised by series and shunt losses. As can be seen in Figure 5, the group with 20 nm thick  $\text{Al}_2\text{O}_3$  shows a significant gain in  $J_{\text{sc}}$  compared to the AL-BSF reference of 2% on average (up to 3% for best neighbor difference). The difference to the  $\text{SiNx}$  reference of 4.3% on average is even larger, illustrating clearly the superiority of the  $\text{Al}_2\text{O}_3$  coating with respect to passivation and, in particular, inversion layer shunting. Unfortunately, all rear passivated groups showed at least 1% lower  $V_{\text{oc}}$  compared to the Al-BSF reference.

### Rear passivation dielectric vs. metallization

The gain in  $J_{\text{sc}}$  for the  $\text{Al}_2\text{O}_3$  group is caused by the improved red response for the  $\text{Al}_2\text{O}_3$  passivated cells as illustrated by

the IQE spectra in Figure 6. Here, the IQE improves at wavelengths larger than 1000nm compared to the Al-BSF reference. The overlap between 800 -1000nm of both cells indicates that the rear surface recombination velocities ( $S_{\text{eff}}$ ), averaged over the full cell area, are equal. This can be deduced as this wavelength range is only influenced by  $\tau_{\text{bulk}}$  and the rear  $S_{\text{eff}}$  [13].

As neighboring wafers are compared and gettering as well as a hydrogenation of the bulk are similar, it is very likely that the bulk life time of both wafers is equal. Assuming a fixed bulk life time allows attributing the gain in  $J_{\text{sc}}$  to a higher internal reflection coefficient at the rear of the cell.

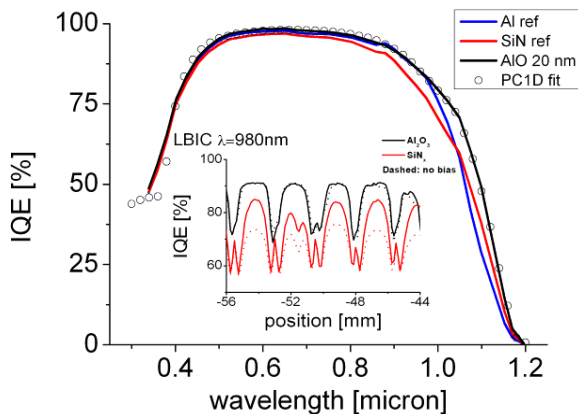


Figure 6, IQE spectra of (neighboring) Al-BSF,  $\text{Al}_2\text{O}_3$  and  $\text{SiN}_x$  passivated mc-Si cells. (Full area and 0.5 Sun bias illumination). Inset: LBIC profile and mapping measured at 980nm of rear side passivated cells with (solid) and without (dashed) bias illumination.

LBIC mapping of the  $\text{Al}_2\text{O}_3$  passivated cell with light of 980nm results in a block-function shaped profile that is independent of bias illumination with a maximum IQE of 91% (inset Figure 6). This demonstrates excellent passivation and absence of parasitic shunting (inversion layer shunting). Fitting the IQE spectrum for the  $\text{Al}_2\text{O}_3$  sample with PC1D allowed verifying the self-consistency between the LBIC and the lifetime measurement. If the local  $S_{\text{eff}}$  value above the  $\text{Al}_2\text{O}_3$  surface is set to the value obtained from the lifetime measurement of 10 cm/s, the IQE of 91% at 980nm can be obtained for a bulk lifetime to 47 $\mu\text{s}$  which is typical for the mc-material used. The fit result of the IQE spectrum is illustrated in Figure 6 and the calculated  $J_{\text{sc}}$  was 0.7% lower and the  $V_{\text{oc}}$  0.4% higher than measured [14]. The rear side passivation of the  $\text{Al}_2\text{O}_3$  passivated cell could be fitted with a rear  $S_{\text{eff}}$  value of 700cm/s at the same bulk lifetime. Based on the LBIC profile a 8% gain (83 to 91%) in IQE could be expected if the contact would passivated as well as the  $\text{Al}_2\text{O}_3$ . Using the PC1D model this gain in IQE corresponds to a gain of 2.6 % in  $J_{\text{sc}}$  and 0.7% in  $V_{\text{oc}}$  which can be considered as an upper limited for the improved rear side.

Based on these findings it can be concluded that the passivation of the cell and thus the cell performance is

limited by the poor passivation at and around the rear metallization. It is furthermore likely that the rear reflection might also increase as poor BSF formation is often accompanied by poor alloy formation. The latter is the prime requisite for good reflection of the fingers. The cause for the poor passivation quality of  $\text{SiN}_x$  is illustrated by the bias dependence and parabola-shaped LBIC profiles in the inset of Figure 6, which are attributed to inversion layer shunt losses [15]. The fact that the  $\text{Al}_2\text{O}_3$  rear passivated cells have on average a 1 % lower voltage as compared to the Al-BSF cells is not fully understood but could well be related to the 2D nature of the rear side which cannot be modeled well in PC1D.

## FUTURE WORK

Further research is required to answer the question why the  $\text{Al}_2\text{O}_3$  samples presented here show such high passivation quality after firing while, in contrast to most reports in literature, no FGA anneal is required. It will be interesting to relate the variation in  $\tau_{\text{eff}}$  caused by chemical pre and thermal post treatments (firing, FGA) as well as variation in film thickness to changes in the surface charge density and surface defect concentration. Methods like CV-MOS, corona charging [3] and second-harmonics generation effects [16] will aid in answering these questions. Furthermore, in order to achieve an efficiency gain for the rear passivated solar cell as compared to the Al-BSF reference, it is apparent that a thicker local BSF as well as a lower rear series resistance is required.

## CONCLUSION

We have shown that a 20nm  $\text{Al}_2\text{O}_3$  film without any capping layer yields satisfactory passivation for the rear passivated PASHA cells based on p-type multi-crystalline wafers. With our process no post treatment (e.g. forming gas anneal) is needed to obtain good  $\text{Al}_2\text{O}_3$  surface passivation. The average rear passivation in completed silicon solar cells must be improved by increasing the BSF depth below the rear metal contacts, which currently limit the cell results below that of the Al-BSF reference. The process flow based on uncapped thin  $\text{Al}_2\text{O}_3$  opens the path towards industrial application of ALD and a concept for high-through put ALD is demonstrated for >3600 wafer/hr. First  $\text{Al}_2\text{O}_3$  layers deposited by this industrial prototype showed excellent passivation quality after firing that is compatible with solar cells with open-circuit voltages up to 720mV.

## ACKNOWLEDGEMENT

We would like to acknowledge Andres Cuevas for assisting in the parameterization and interpretation of the lifetime measurements. This work was partially financed by the Agentschap NL, in the project Newton (EOS-KTO program project T09000212).

## REFERENCES

- [1] J. Benick, A. Richter, M. Hermle, and S. W. Glunz, "Thermal stability of the  $\text{Al}_2\text{O}_3$  passivation on p-type silicon surfaces for solar

- cell applications" *Phys. Status Solidi RRL*, **3**, 233 (2009).
- [2] J. Schmidt, A. Merkle, R. Brendel, B. Hoex, M. C. C. van der Sanden, and W. M. M. Kessels, "Surface passivation of high-efficiency silicon solar cells by atomic-layer-deposited Al<sub>2</sub>O<sub>3</sub>" *PROGRESS IN PHOTOVOLTAICS: RESEARCH AND APPLICATIONS*, vol. **16**, no. 6, pp. 461-466, 2008.
- [3] B. Hoex, J. Schmidt, P. Pohl, M. C. M. van de Sanden, and W. M. M. Kessels, "Silicon surface passivation by atomic layer deposited Al<sub>2</sub>O<sub>3</sub>", *J. Appl. Phys.*, **104**, 4, (2008) 044903/1.
- [4] G. Dingemans, M. C. C. van der Sanden, and W. M. M. Kessels, "Influence of the Deposition Temperature on the c-Si Surface Passivation by Al<sub>2</sub>O<sub>3</sub> Films Synthesized by ALD and PECVD", *Electrochemical and Solid-State Letters*, **13**, 3 2009, pp. H76-79H.
- [5] S. Dauwe, L. Mittelstadt, A. Metz, and R. Hezel, "Experimental evidence of parasitic shunting in silicon nitride rear surface passivated solar cells", *Prog. Photovoltaics*, **10**, 4, 2002, pp. 271-278.
- [6] I. Cesar, E. E. Bende, G. Galbiati, L. Janßen, A. A. Mewe, P. Manshanden, A. W. Weeber, and J. H. Bultman, "Parasitic shunt losses in all-side SiN<sub>x</sub> passivated mc-Si solar cells" Proc. 24<sup>th</sup> EUPVSEC 2009.
- [7] T. T. Li and A. Cuevas, "Effective surface passivation of crystalline silicon by rf sputtered aluminum oxide", *Phys. Status Solidi RRL*, **3**, 5, 2009, pp. 160-162.
- [8] G. Dingemans, M. C. C. van der Sanden, and W. M. M. Kessels, "Influence of the Deposition Temperature on the c-Si Surface Passivation by Al<sub>2</sub>O<sub>3</sub> Films Synthesized by ALD and PECVD", *Electrochemical and Solid-State Letters*, **13**, 3 2009, pp. H76-79H
- [9] J. Schmidt, B. Veith, and R. Brendel, "Effective surface passivation of crystalline silicon using ultrathin Al<sub>2</sub>O<sub>3</sub> films and Al<sub>2</sub>O<sub>3</sub>/SiN<sub>x</sub> stacks", *Phys. Status Solidi RRL* **3**, 9, 2009, pp. 287-289.
- [10] A. Stassen, M. Koppes, and J. Hoogboom, "Further improvements in surface modification of MC silicon solar cells: comparison of different post-PSG cleans for inline emitters", *Photovoltaic international*, **6**, 2009, p. 71.
- [11] I. Cesar, I. G. Romijn, D. M. Borsa, G. Galbiati, N. J. C. M. van der Borg, E. E. Bende, and A. W. Weeber, "Benchmark of open rear side solar cell with improved Al-BSF process at ECN" Proc. 23<sup>th</sup> EUPVSEC, 2008.
- [12] A. Cuevas and R. Sinton, "QSS-Model V3," 2010.
- [13] P. A. Basore and D. A. Clugstone, "PC1D v5.5," 2000.
- [14] "Other fit parameters used were: R<sub>in</sub> front and rear of 94 and 92%, Front SRV of 6x10<sup>5</sup> cm/s and the emitter was modeled with an error function (N<sub>a,peak</sub> = 5x10<sup>19</sup> cm<sup>-3</sup>, 0.11 micron), wafer thickness of 188µm, base resistivity 1ohm.cm. No parallel circuits elements were used in the model."
- [15] S. Dauwe, Ph.D. Thesis, "Low-Temperature Surface Passivation of Crystalline and its Application to the Rear Side of Solar Cells." ISFH, 2004.
- [16] J. J. H. Gielis, B. Hoex, M. C. M. van de Sanden, and W. M. M. Kessels, *J. Appl. Phys.*, vol. **104**, p. 073701, 2008.